Supporting Information

Thermosensitive Hydrogel-based, High Performance and Flexible Sensor for Multi-functional E-skin

Dongdong Lu[a,b], Mingning Zhu[c], Xiaoyuan Li[d], Zilong Zhu[a], Xin Lin[a], Chuanfei Guo[a*] and Xiaodong Xiang[a,c*]

a. Department of Materials Science and Engineering, Southern University of Science and Technology, Shenzhen, Guangdong 518000, China

b. School of Physical Sciences, Great Bay University, Dongguan, 523000, China

c. Academy for Advanced Interdisciplinary Studies, Southern University of Science and Technology, 1088 Xueyuan Avenue, Shenzhen 518055, P. R. China

d. Department of Chemistry, The Hong Kong University of Science and Technology, Clearwater Bay, Kowloon, Hong Kong S.A.R, China

*Corresponding authors:

E-mail: guocf@sustech.edu.cn

E-mail: xiangxd@sustech.edu.cn

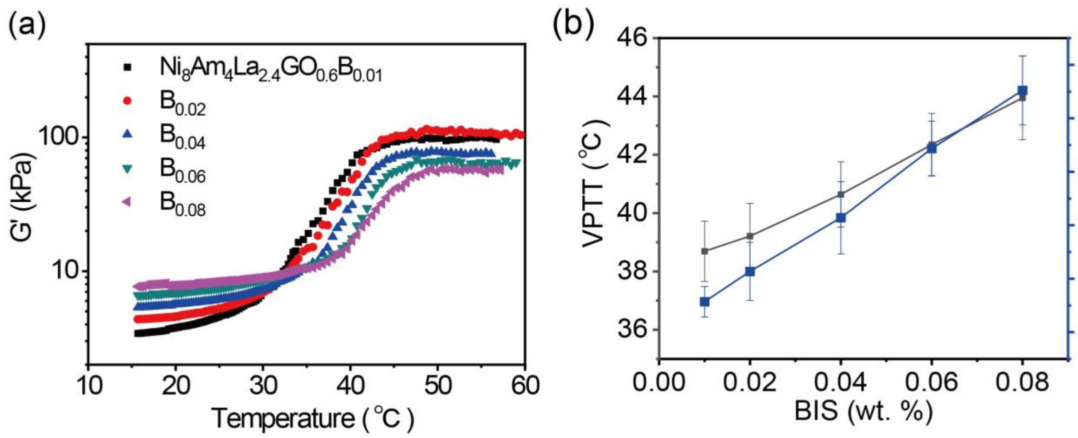

Fig. S1. **(a)** Temperature-sweep rheology data for $Ni_{60}Am_{40}La_{2.4}GO_{0.6}B_{s}$. **(b)** G' and *VPTT* values vs. BIS content for the hydrogels from (a).

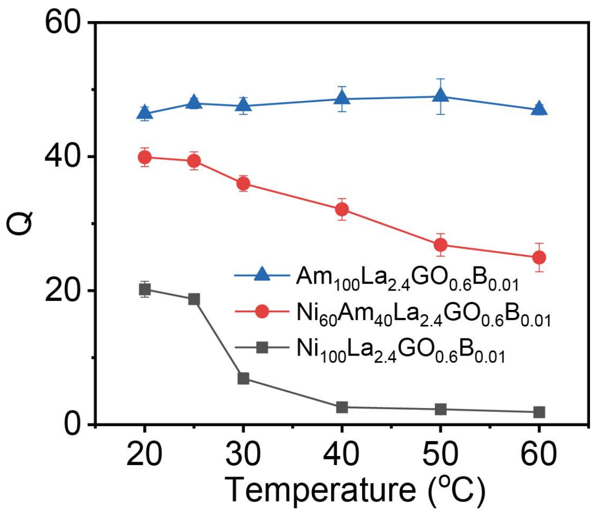

Fig. S2. Temperature-dependent swelling ratio (*Q*) of $Am_{100}La_{2.4}GO_{0.6}B_{0.01}$, $Ni_{60}Am_{40}La_{2.4}GO_{0.6}B_{0.01}$ and $Ni_{100}La_{2.4}GO_{0.6}B_{0.01}$.

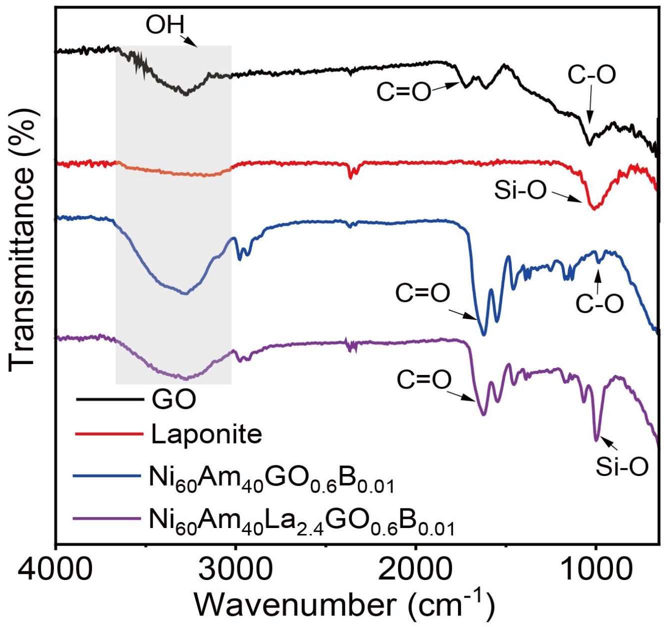

Fig. S3. FTIR spectrum of GO, laponite, $Ni_{60}Am_{40}GO_{0.6}B_{0.01}$ and $Ni_{60}Am_{40}La_{2.4}GO_{0.6}B_{0.01}$.

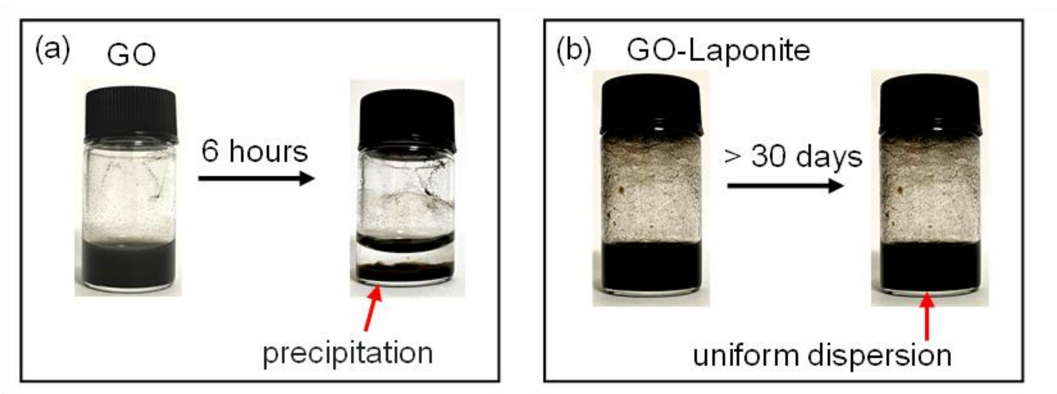

Fig. S4. Images of GO dispersion (a) and mixture of GO and laponite (b) settled after 6 hours and over than a month.

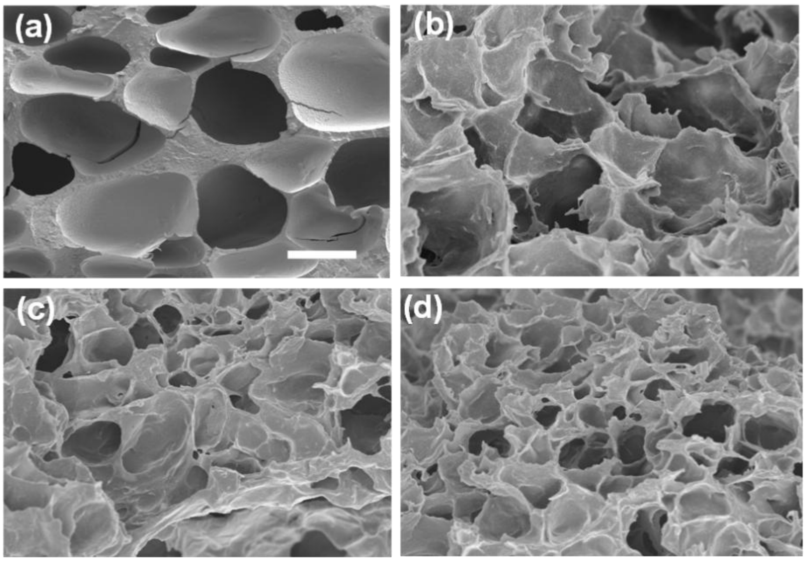

Fig. S5. SEM images of $Ni_{60}Am_{40}B_{0.01}$, $Ni_{60}Am_{40}GO_{0.6}B_{0.01}$, $Ni_{60}Am_{40}La_{2.4}B_{0.01}$ and $Ni_{60}Am_{40}La_{2.4}GO_{0.6}B_{0.01}$. The scale bar in (a) is 50μm and applied to all images.

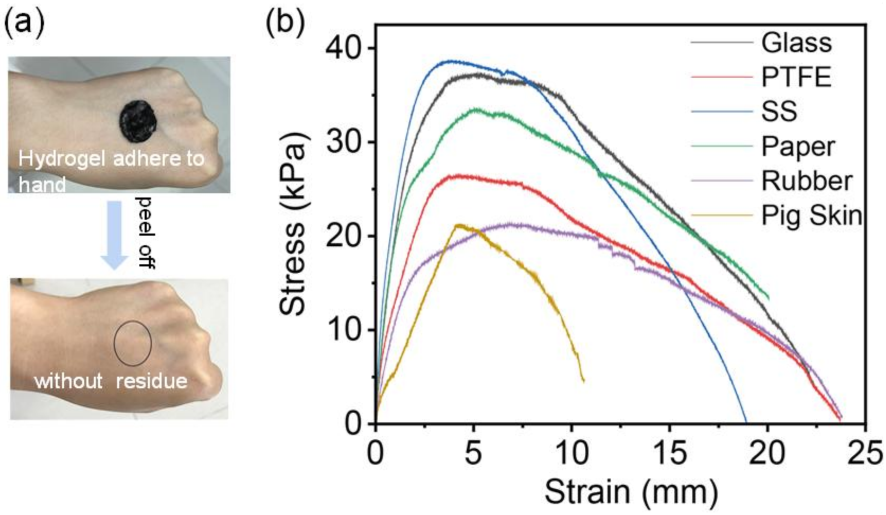

Fig. S6. (a) Tissue adhesiveness of the $Ni_{60}Am_{40}La_{2.4}GO_{0.6}B_{0.01}$ hydrogel on the author's hand. (b) The adhesive curve of hydrogel to different substrates (glass, PTFE, plastic, paper, stainless steel (SS) and pig skin). All data were measured at 25 °C.

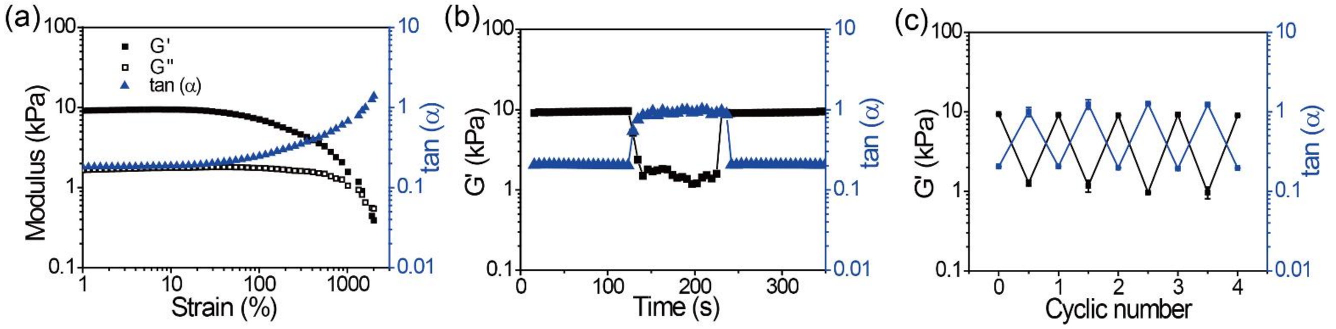

Fig. S7. (a) Rheological strain and **(b)** dynamic alternating strain-time sweeping measurements of the $Ni_{60}Am_{40}La_{2.4}GO_{0.6}B_{0.01}$. **(c)** the change of *G′* value and *tan δ* $Ni_{60}Am_{40}La_{2.4}GO_{0.6}B_{0.01}$ with cyclic alternating strain between 1000% and 1%.

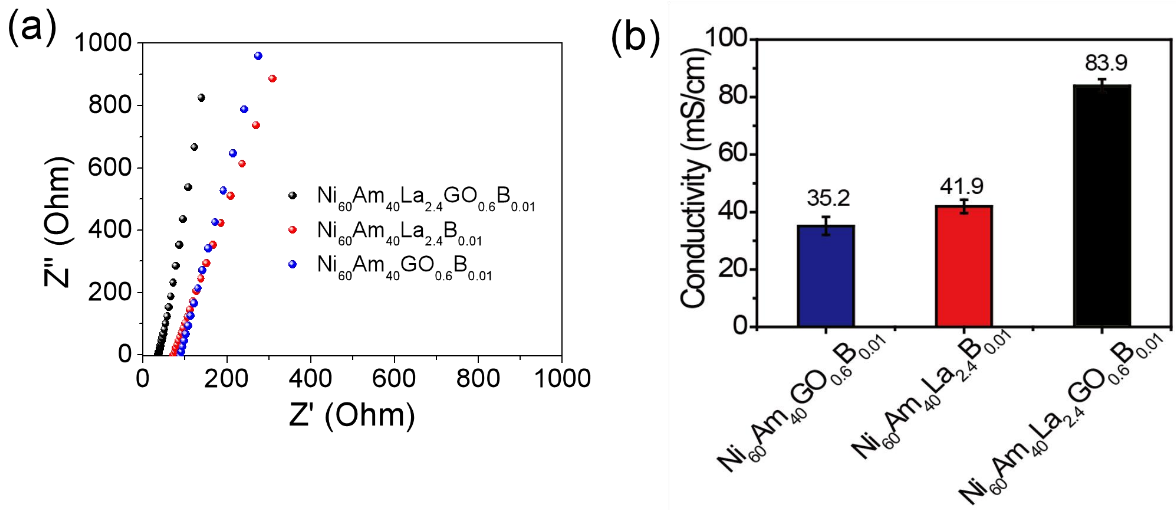

Fig. S8. Conductivity of $Ni_xAm_yLa_zGO_nB_s$ at 25 °C

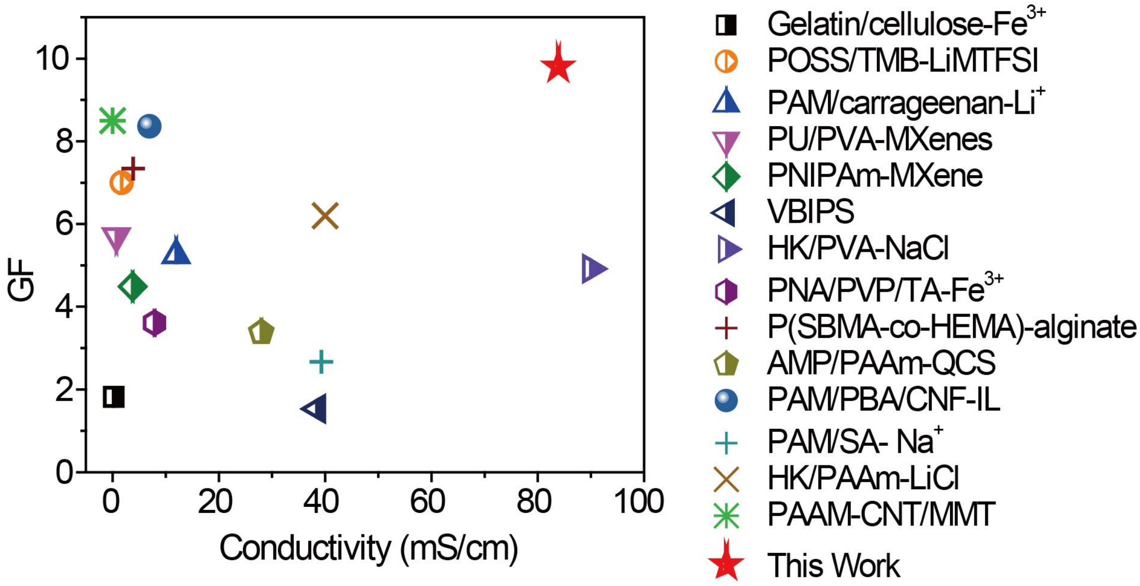

Fig. S9. Comparsion of *GF* and conductivity of $Ni_{60}Am_{40}La_{2.4}GO_{0.6}B_{0.01}$ to reported hydrogels sensor. The detailed data was listed in Table S1.

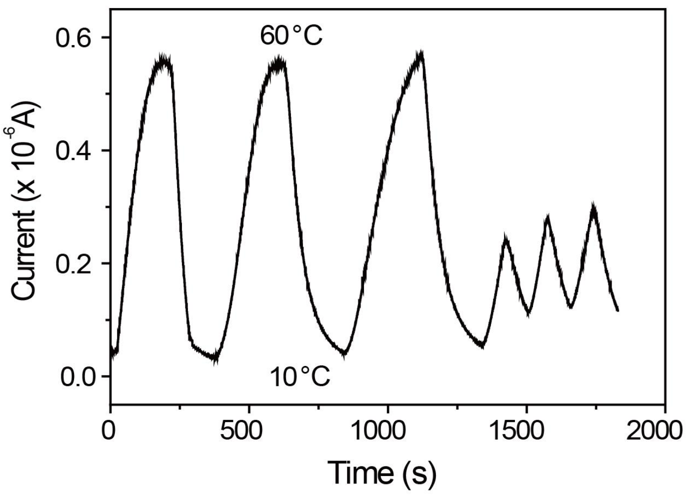

Fig. S10. Time-dependent of current for putting the $Ni_{60}Am_{40}La_{2.4}GO_{0.6}B_{0.01}$ hydrogel from 10℃ to 60℃ reversely. The former three cycle was changing the external temperature from 10℃ to 60℃ (or from 60℃ to 10℃) and kept for 200 s. The latter three cycle is kept for 80 s.

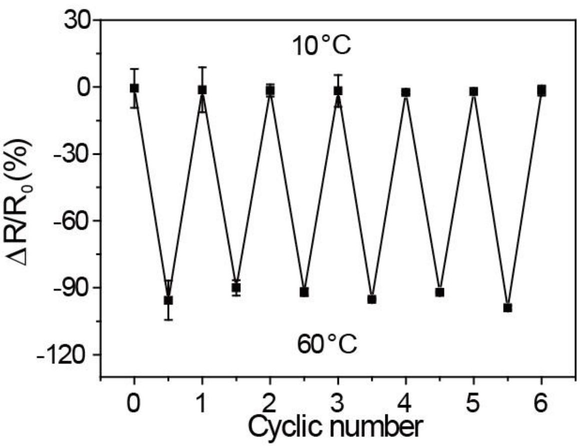

Fig. S11. Re-cyclic test of Resistance changes for $Ni_{60}Am_{40}La_{2.4}GO_{0.6}B_{0.01}$ at 10°C and 60°C.

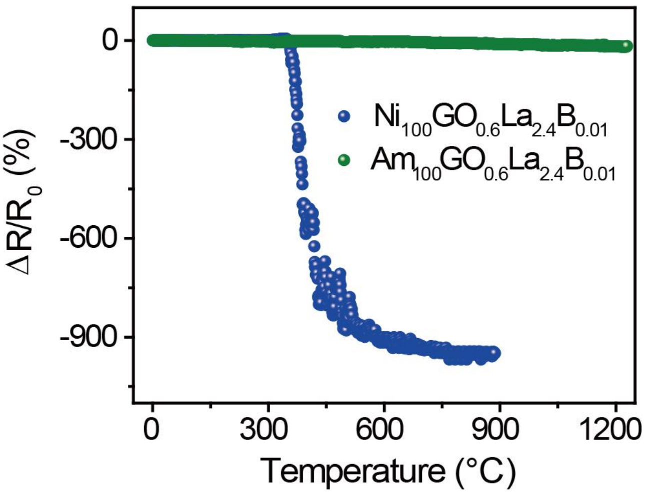

Fig. S12. Resistance changes *vs*. temperature for $Ni_{100}GO_{0.6}La_{2.4}B_{0.01}$ and $Am_{100}GO_{0.6}La_{2.4}B_{0.01}$

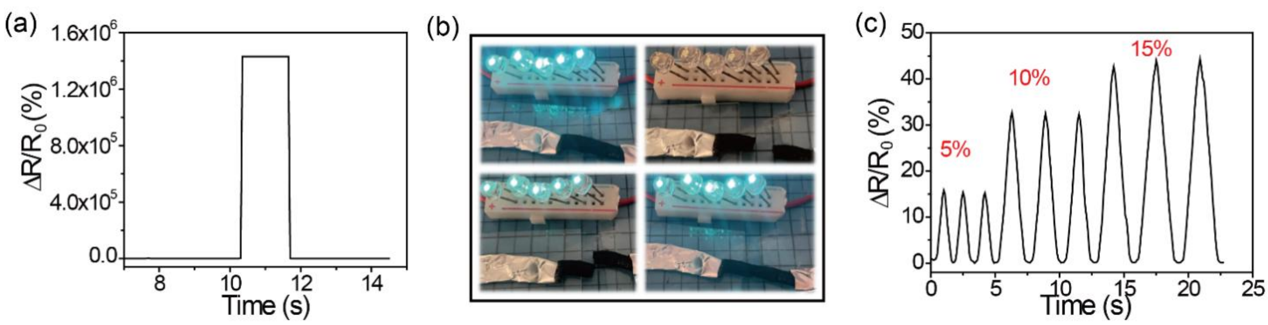

Fig. S13. **(a)** The conductive responses and **(b)** images of the hydrogel when cutting and self-healing **(c)** Real-time relative resistance changes of the self-healed $Ni_{60}Am_{40}La_{2.4}GO_{0.6}B_{0.01}$ under different strains.

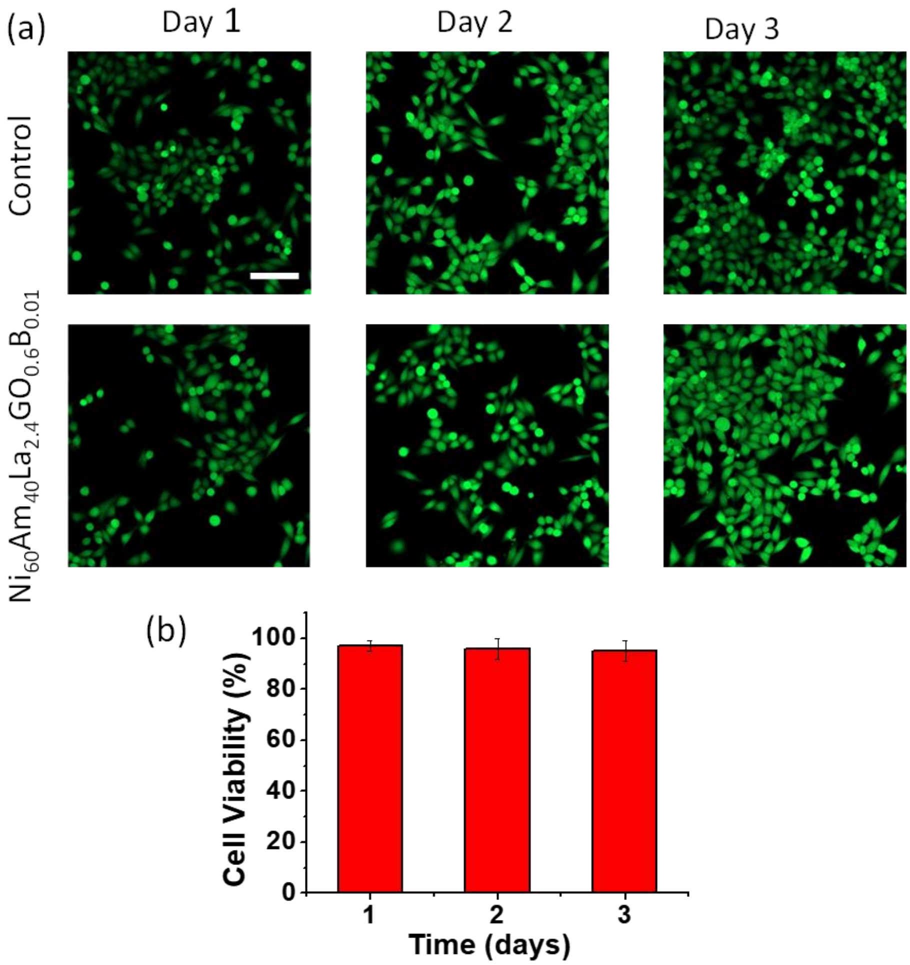

Fig. S14. **(a)** Live/Dead cell assay and **(b)** cell viability calculated from MTT assay for the $Ni_{60}Am_{40}La_{2.4}GO_{0.6}B_{0.01}$ gel. The control is the PBS solution. The scale bar in (a) is 100 µm.

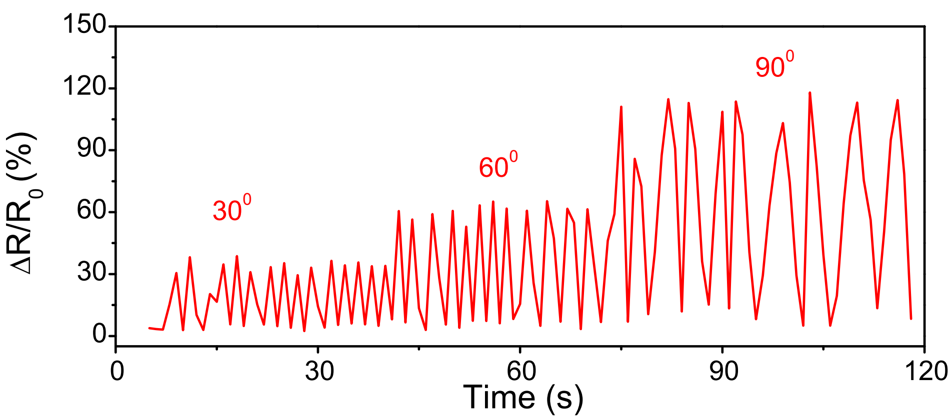

Fig. S15. Finger bending at 30°, 60° and 90°.

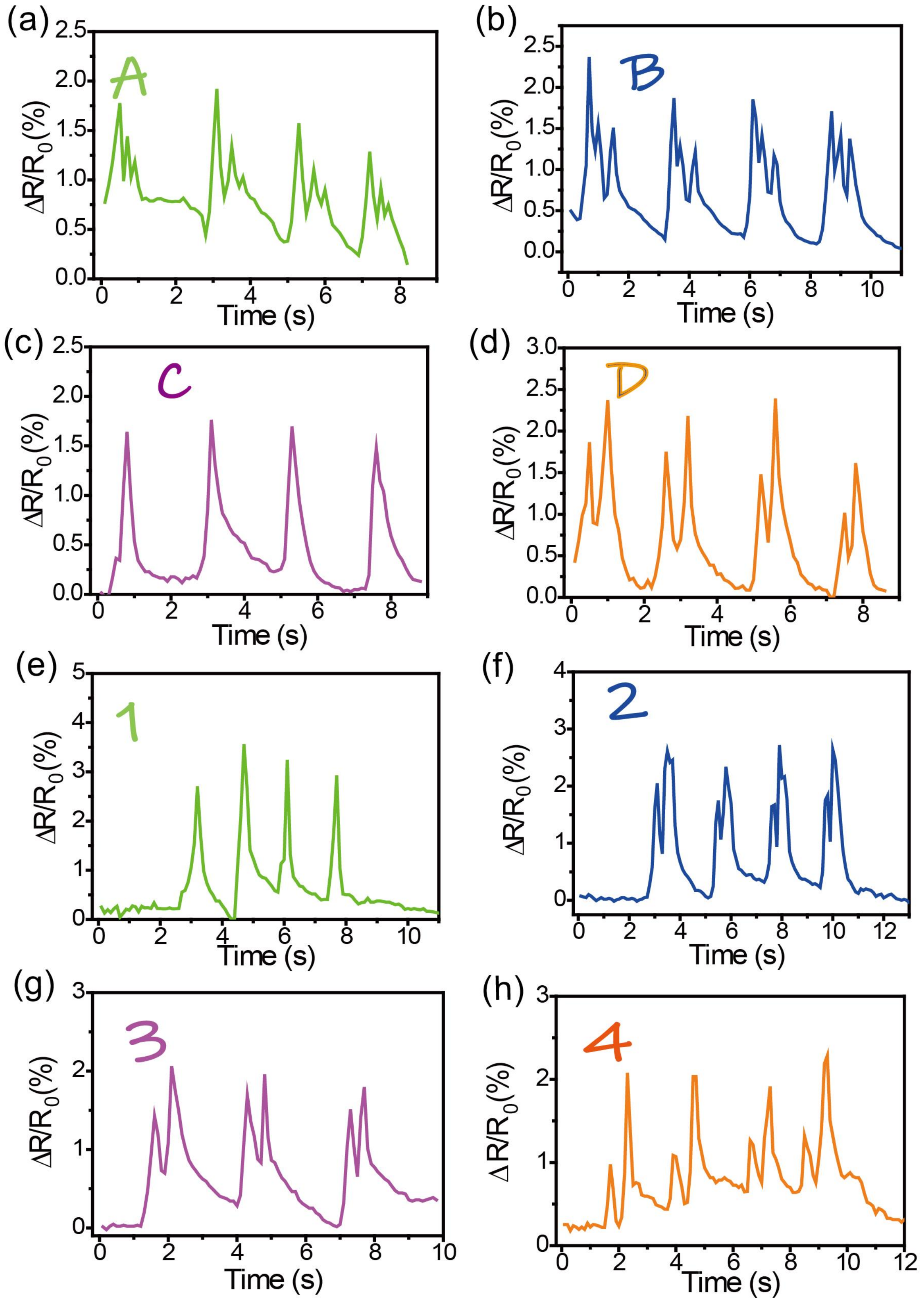

Fig. S16. Real-time relative resistance changes of "A", "B", "C", "D" and "1", "2", "3", "4" in the same handwriting.

Table S1. Performance comparison for conductivity and *GF* with reported sensor.

Sample Name	Conductivity(mS/cm)	*GF*	Reference
$Ni_{60}Am_{40}La_{2.4}GO_{0.6}B_{0.01}$	83.9	9.8	This Work
Gelatin/cellulose/Fe3+	0.3	1.8	1
POSS/TMB-LiMTFSI	1.7	7.0	2
PAM/carrageenan-Li+	12.0	5.3	3
PU/PVA-MXenes	0.7	5.7	4
PNIPAm-MXene	3.8	4.5	5
VBIPS	38.5	1.5	6
HK/PVA-NaCl	90.0	4.9	7
PNA/PVP/TA-Fe3+	7.9	3.6	8
P(SBMA-co-HEMA)-alginate	3.9	7.3	9
AMP/PAAm-QCS	28.0	3.4	10
PAM/PBA/CNF-IL	6.9	8.4	11
PAM/SA- Na+	39.3	2.7	12
HK/PAAm-LiCl	40.0	6.2	13
PAAM-CNT/MMT	0.01	8.5	14

Reference

1. Fu, H. C.; Wang, B.; Li, J. P.; Xu, J.; Li, J.; Zeng, J. S.; Gao, W. H.; Chen, K. F., A self-healing, recyclable and conductive gelatin/nanofibrillated cellulose/Fe3+ hydrogel based on multi-dynamic interactions for a multifunctional strain sensor. *Mater. Horiz.* **2022,** *9* (5).

2. Ou, Y.; Zhao, T. T.; Zhang, Y.; Zhao, G. H.; Dong, L. J., Stretchable solvent-free ionic conductor with self-wrinkling microstructures for ultrasensitive strain sensor. *Mater. Horiz.* **2022,** *9* (6), 1679-1689.

3. Wu, Z. X.; Shi, W. X.; Ding, H. J.; Zhong, B. Z.; Huang, W. X.; Zhou, Y. B.; Gui, X. C.; Xie, X.; Wu, J., Ultrastable, stretchable, highly conductive and transparent hydrogels enabled by salt-percolation for high-performance temperature and strain sensing. *J. Mater. Chem. C* **2021,** *9* (39), 13668-13679.

4. Liu, H. D.; Du, C. F.; Liao, L. L.; Zhang, H. J.; Zhou, H. Q.; Zhou, W. C.; Ren, T. N.; Sun, Z. C.; Lu, Y. F.; Nie, Z. T.; Xu, F.; Zhu, J. X.; Huang, W., Approaching intrinsic dynamics of MXenes hybrid hydrogel for 3D printed multimodal intelligent devices with ultrahigh superelasticity and temperature sensitivity. *Nat. Commun.* **2022,** *13* (1).

5. Hao, F.; Wang, L. Y.; Chen, B. L.; Qiu, L.; Nie, J.; Ma, G. P., Bifunctional Smart Hydrogel Dressing with Strain Sensitivity and NIR-Responsive Performance. *ACS Appl. Mater. Interfaces* **2021,** *13* (39), 46938-46950.

6. Zheng, S. Y.; Mao, S. H.; Yuan, J. F.; Wang, S. B.; He, X. M.; Zhang, X. N.; Du, C.; Zhang, D.; Wu, Z. L.; Yang, J. T., Molecularly Engineered Zwitterionic Hydrogels with High Toughness and Self-Healing Capacity for Soft Electronics Applications. *Chem.*

Mater. **2021,** *33* (21), 8418-8429.

7. Gao, Y.; Gu, S.; Jia, F.; Gao, G. H., A skin-matchable, recyclable and biofriendly strain sensor based on a hydrolyzed keratin-containing hydrogel. *J. Mater. Chem. A* **2020,** *8* (45), 24175-24183.

8. Pang, Q.; Hu, H. T.; Zhang, H. Q.; Qiao, B. B.; Ma, L., Temperature-Responsive Ionic Conductive Hydrogel for Strain and Temperature Sensors. *ACS Appl. Mater. Interfaces* **2022,** *14*, 26536-26547.

9. Wei, H.; Wang, Z. W.; Zhang, H.; Huang, Y. J.; Wang, Z. B.; Zhou, Y.; Xu, B. B.; Halila, S.; Chen, J., Ultrastretchable, Highly Transparent, Self-Adhesive, and 3D-Printable Ionic Hydrogels for Multimode Tactical Sensing. *Chem. Mater.* **2021,** *33* (17), 6731-6742.

10. Zhang, Q.; Liu, X.; Duan, L. J.; Gao, G. H., A DNA-inspired hydrogel mechanoreceptor with skin-like mechanical behavior. *J. Mater. Chem. A* **2021,** *9* (3), 1835-1844.

11. Yao, X.; Zhang, S.; Qian, L.; Wei, N.; Nica, V.; Coseri, S.; Han, F., Super Stretchable, Self-Healing, Adhesive Ionic Conductive Hydrogels Based on Tailor-Made Ionic Liquid for High-Performance Strain Sensors. *Adv. Funct. Mater.* **2022,** *32* (33), 2204565.

12. Lu, X. Y.; Si, Y.; Zhang, S. C.; Yu, J. Y.; Ding, B., In Situ Synthesis of Mechanically Robust, Transparent Nanofiber-Reinforced Hydrogels for Highly Sensitive Multiple Sensing. *Adv. Funct. Mater.* **2021,** *31* (30).

13. Gao, Y.; Gu, S.; Jia, F.; Wang, Q.; Gao, G. H., "All-in-one" hydrolyzed keratin

protein-modified polyacrylamide composite hydrogel transducer. *Chem. Eng. J.* **2020,** *398*.

14. Sun, H. L.; Zhao, Y.; Jiao, S. L.; Wang, C. F.; Jia, Y. P.; Dai, K.; Zheng, G. Q.; Liu, C. T.; Wan, P. B.; Shen, C. Y., Environment Tolerant Conductive Nanocomposite Organohydrogels as Flexible Strain Sensors and Power Sources for Sustainable Electronics. *Adv. Funct. Mater.* **2021,** *31* (24).